

Order-driven contribution to the planar Hall effect in Fe₃Si thin films

M. Bowen,* K.-J. Friedland, J. Herfort, H.-P. Schönherr, and K. H. Ploog
 Paul Drude Institute for Solid State Electronics, Hausvogteiplatz 5-7, 10117 Berlin, Germany
 (Received 3 February 2005; published 4 May 2005)

We report on an intrinsic origin to the planar Hall effect through experiments on the Heusler alloy Fe_{3+x}Si_{1-x} in the range $-0.08 \leq x \leq +0.06$. Both structural ordering around exact Fe₃Si stoichiometry and thermally regulated magnetic ordering of interpenetrating fcc Fe sublattices drive the planar Hall effect from a conventional to an ordered intrinsic magnetotransport regime. The transition is marked by a change in sign of ρ_{xy} but not of $\Delta\rho_{xx}$. A microscopic model which extends anisotropic magnetoresistance theory correctly describes this regime.

DOI: 10.1103/PhysRevB.71.172401

PACS number(s): 75.47.Np, 72.15.Eb, 73.43.-f, 75.50.Bb

Both the anomalous Hall effect¹ (AHE) and anisotropic magnetoresistance² (AMR)—studied intensively over the past several decades—relate to the magnetization of a ferromagnetic thin film in an external magnetic field applied perpendicular and parallel to the film plane, respectively. An early intrinsic description ascribed the anomalous Hall resistivity to a spin-orbit interaction of spin-polarized conduction electrons,³ while extrinsic models involved scattering potentials due to impurities and defects.^{4,5}

The past five years have seen a surge in research on an intrinsic origin to the AHE. According to a recent theory⁶ on the prototypical ferromagnet Fe, the AHE arises due to conduction of carriers from a very narrow portion of the Fermi surface which is split by the spin-orbit interaction. The near degeneracy of spin up and spin down states at such points in the band structure may thus induce a nontrivial spin topology throughout the ferromagnet's lattice. Due to a Berry phase^{7,8} connection of wavefunctions, this leads to a transverse resistivity, which is intrinsic to the ferromagnetic material. However, while the AHE and the planar Hall effect (PHE) both originate from the spin-orbit interaction,⁹ the PHE has not yet been described in a similar framework, despite a conjunction of PHE experiments¹⁰ on and AHE Berry phase theory¹¹ of dilute magnetic semiconductors. While PHE measurements on Fe have evidenced a deviation from AMR theory,^{9,12} a Berry phase description was not applied.

In this paper, we present experimental results on Fe_{3+x}Si_{1-x} thin films with DO₃ crystal structure and composition x near Fe₃Si [see Fig. 1(a)], which also reveal an additional contribution to the PHE as compared to the straightforward AMR model. A microscopic model functionally reproduces this PHE term, which we ascribe to topological defects in the spin density distribution. In support of our model, both thermal and structural disorder drive magnetotransport into a conventional regime by destroying the coherence of spin fluctuations between Fe sublattices.

Epitaxial Fe_{3+x}Si_{1-x} thin films of high crystalline and interfacial quality were grown by molecular-beam epitaxy on GaAs(001) substrates.¹³ With thicknesses in the 30–50 nm range, these fully strained films are sufficiently thick to quench any significant uniaxial anisotropy.¹⁴ Fe_{3+x}Si_{1-x} films with nearly exact stoichiometry $x=0$ are almost lattice-matched to the GaAs(001) substrate and exhibit a nearly complete magnetization remanence along a [100] easy axis as well as coercive fields of 1 Oe.¹⁴

Within AMR and AHE theory, the electric field \mathbf{E} resulting from a current density \mathbf{j} applied through a ferromagnetic thin film with magnetization vector of unit length \mathbf{m} is given by

$$\mathbf{E} = \rho_{\parallel}\mathbf{j} + (\rho_{\parallel} - \rho_{\perp})(\mathbf{j} \cdot \mathbf{m})\mathbf{m} + \rho_{HS}(\mathbf{m} \times \mathbf{j}). \quad (1)$$

With sample resistivities ρ_{\parallel} and ρ_{\perp} for configurations of current parallel and perpendicular to \mathbf{m} , respectively, the first term embodies in part longitudinal magnetoresistance and the second one AMR theory. ρ_{HS} describes the normal Hall effect and the AHE resulting from the out-of-plane component of magnetization. Thus, upon rotating a film with a single magnetization domain in a fixed in-plane magnetic field, the longitudinal and transverse resistivities $\Delta\rho_{xx}$ and ρ_{xy}^{AMR} evolve as

$$\Delta\rho_{xx} = (\rho_{\parallel} - \rho_{\perp})\cos^2(\theta_M), \quad (2)$$

$$\rho_{xy}^{AMR} = \frac{1}{2}(\rho_{\parallel} - \rho_{\perp})\sin(2\theta_M), \quad (3)$$

where θ_M denotes the angle between magnetization and current. ρ_{xy}^{AMR} is also called the planar Hall effect.

Magnetotransport experiments in the planar Hall geometry were performed on rectangular samples with Ohmic contacts such that a homogeneous current was directed along the [-110] hard axis. In this crystallographic direction, the angle of in-plane applied magnetic field θ_H is 0. When the magnetic field is directed along an easy magnetization axis, i.e. for $\theta_H=45^\circ$, the directions of applied field and magnetization coincide ($\theta_H=\theta_M$). As the sample is rotated away from $\theta_H=45^\circ$, θ_M begins to lag behind θ_H . Figure 2 presents the evolution of ρ_{xx} and ρ_{xy} with θ_H on a nearly stoichiometric Fe_{3+x}Si_{1-x} sample ($x=+0.01$; 44 nm thick) at $T=77$ K and $T=300$ K. For an applied field $H=25$ Oe which does not overcome the film's fourfold anisotropy energy,¹⁴ sweeping θ_H through a hard axis induces a jump in θ_M toward the next easy axis and consequently a kink (jump) in ρ_{xx} (ρ_{xy}) data. Such behavior indicates single-domain magnetization reversal. As the crucial observation of this paper, an inversion in the angular traces of ρ_{xy} has occurred between $T=77$ K and $T=300$ K, while the angular dependence of ρ_{xx} remains unchanged. The implied sign change of $\rho_{xy}(\theta_H)$ takes place at

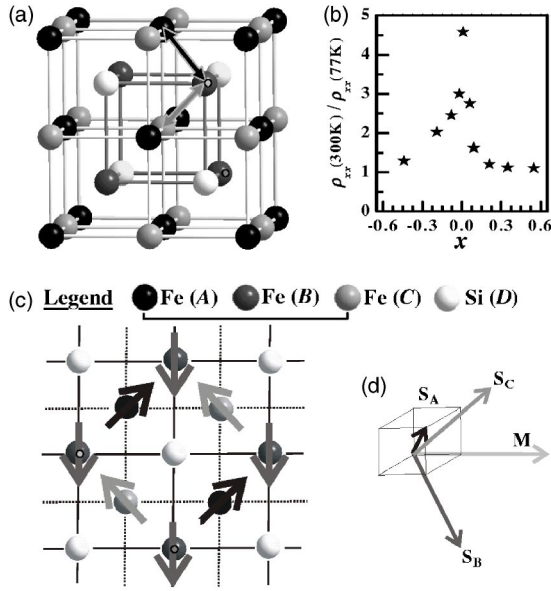


FIG. 1. (a) $D0_3$ structure of Fe_3Si . Arrows indicate magnetic interactions between $\text{Fe}(B)$ and $\text{Fe}(A,C)$ sites. (b) Evolution of $\rho_{xx}(300\text{ K})/\rho_{xx}(77\text{ K})$ with x for $\text{Fe}_{3+x}\text{Si}_{1-x}$. (c) One spin configuration in a (100) plane for magnetization $\mathbf{M}\parallel[100]$, with chirality $\chi>0$ due to noncoplanar orientations of $\text{Fe}(A,B,C)$ spins which compose \mathbf{M} as schematized in (d).

$T_{\text{ord}}=251\text{ K}$ for this sample and persists even for a moderate applied field which has overcome the fourfold anisotropy energy. Significantly nonstoichiometric samples do not show this sign change.

Figure 3 presents magnetic field sweeps of ρ_{xx} and ρ_{xy} at a fixed angle θ_H away from the hard axis at $T=300\text{ K}$. Our measurements on Fe_3Si down to $T=77\text{ K}$ show that $\rho_{\parallel}<\rho_{\perp}$, an unusual but not unique result.² As the field is lowered, all ρ_{xx} curves [Fig. 3(a)] converge toward the same low-field resistivity, which reflects the rotation of sample magnetization toward an easy axis as identified by the measurement for $\theta_H=45^\circ$. Given Eq. (2), one cannot distinguish between different easy axes from ρ_{xx} data. Correspondingly, ρ_{xy} data

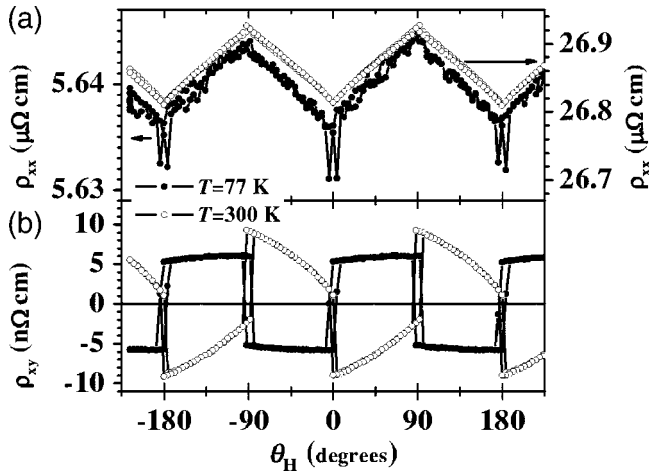


FIG. 2. (a) ρ_{xx} and (b) ρ_{xy} vs θ_H at $T=77\text{ K}$ (dots) and $T=300\text{ K}$ (circles) for a sample with $x=+0.01$ at $H=25\text{ Oe}$.

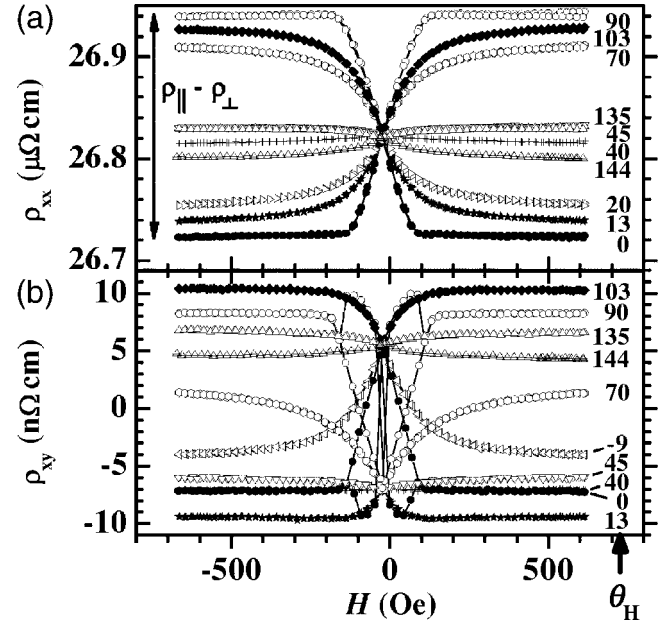


FIG. 3. (a) ρ_{xx} and (b) ρ_{xy} vs applied field H for specific angles θ_H (in degrees), at $T=300\text{ K}$ for $x=+0.01$.

[Fig. 3(b)] converge to the $45^\circ/135^\circ$ points in a vanishing applied field, and ρ_{xy} may exhibit two switching events as θ_M jumps from one easy axis to another during magnetization reversal. However, the $45^\circ/135^\circ$ orientations of magnetization do not represent an extremum as expected within AMR theory from Eq. (3).

To simplify the complex magnetization behavior presented in Figs. 2 and 3, we assume to first order that ρ_{xx} fulfills AMR theory and extract θ_M ¹² from Eq. (2). We may then plot ρ_{xy} as a function of θ_M as shown in Fig. 4 for $T=300\text{ K}$ and $T=77\text{ K}$. Relative to AMR theory, $\rho_{xy}(\theta_M)$ also exhibits the expected fourfold anisotropic behavior but is phase-shifted by $\Delta\theta_M(T=300\text{ K})=-22.5^\circ$ and $\Delta\theta_M(T=77\text{ K})=+95^\circ$ with respect to these axes. Furthermore, $\Delta\rho_{xy}(\theta_M)$ is generally much lower than the value predicted by AMR theory. We therefore introduce¹² a *compensating* term to ρ_{xy}

$$\rho_{xy} = \sigma_{xy}^{\text{AMR}} + \rho_{xy}^{\text{Comp}} = \frac{1}{2}(\rho_{\parallel} - \rho_{\perp})\sin(2\theta_M) + \rho_{\text{Comp}}\frac{1}{2}\sin(2\theta_M + \theta), \quad (4)$$

which can correct AMR theory above and below T_{ord} (see insets of Fig. 4) using $T=300\text{ K}$: $\rho_{\text{Comp}}=-0.95(\rho_{\parallel}-\rho_{\perp})$, $\theta=2.1^\circ$; $T=77\text{ K}$: $\rho_{\text{Comp}}=-1.49(\rho_{\parallel}-\rho_{\perp})$, $\theta=-3.3^\circ$.

Effects due to domain wall boundaries, atomic disorder, and electron localization could explain our results within AMR theory only if both ρ_{xx} and ρ_{xy} behaved similarly. Also, AMR theory cannot account for $|\rho_{xy}|\ll\rho_{\parallel}-\rho_{\perp}$. A change in sign of the cubic anisotropy constant K_1 (Ref. 15) may be ruled out since the angular position of the jump in ρ_{xy} remains unchanged. A systematic error in the in-plane angular position has been corrected to within $\pm 2^\circ$, and the fourfold symmetry of ρ_{xy} jumps precludes any dominant contribution

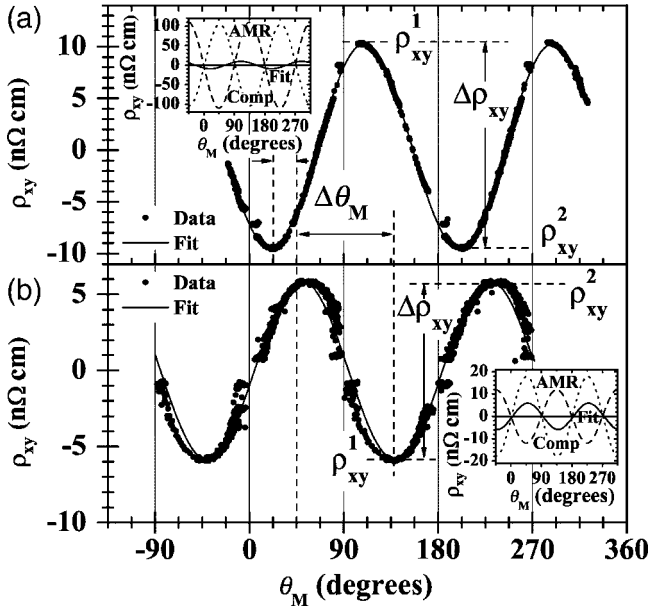


FIG. 4. ρ_{xy} vs θ_M obtained within AMR theory from ρ_{xx} data, at (a) $T=300$ K and (b) $T=77$ K, and fit to Eq. (4) for $x=+0.01$. Insets: ρ_{xy}^{Comp} , ρ_{xy}^{AMR} , and fit vs θ_M .

from uniaxial anisotropy, in agreement with other measurements.¹³ Any small out-of-plane misalignment would induce an antisymmetric angular response from the AHE and was carefully avoided. An intrinsic out-of-plane magnetization was not observed. In addition, such considerations are already excluded through the data analysis contained in Fig. 4, which now narrows the problem exclusively to the dependence of the PHE on θ_M . Altogether, our results demonstrate the existence of an additional contribution to the PHE.

Toward a microscopic model for the additional PHE observed in ordered Fe_3Si with $D0_3$ symmetry, we analyze the ensemble of collective spin fluctuations on the different sublattices given the intra-lattice spin density distribution¹⁶ and a two-spin interaction between the Fe(A,C) and Fe(B) sublattices.¹⁷ The Fe(B) site lies in a cubic magnetic environment of Fe(A,C) sites, so that its spin is unconstrained in rotation. In contrast, the inversion symmetry of the Fe(A,C) spin sublattices is broken due to a tetrahedral Fe(B) environment, resulting in preferred spin orientations. Without any loss of generality to our model, we assume that their on-site spins tend to align along $\langle 111 \rangle$ directions containing the magnetically stronger Fe(B) nearest neighbor sites [see arrows in Fig. 1(a)]. Using this constraint, configurations of spins $\mathbf{S}_A, \mathbf{S}_B, \mathbf{S}_C$ at lattice sites Fe(A), Fe(B), and Fe(C) may be found such that the spin chirality $\chi_{ABC} = \mathbf{S}_A \cdot (\mathbf{S}_B \times \mathbf{S}_C) \neq 0$. An example of such a collective spin configuration, which conserves the orientation of mean magnetization $\mathbf{m} \parallel [100]$ and yields $\chi_{ABC} > 0$, is demonstrated in Figs. 1(c) and 1(d). We thus describe collective spin fluctuations in a normal ferromagnet with no frustrated steady spin state.

Spin chirality acts as the gauge flux for the charged carriers which evolve in the background of fluctuating spins, thus describing the AHE as due to a Berry phase connection

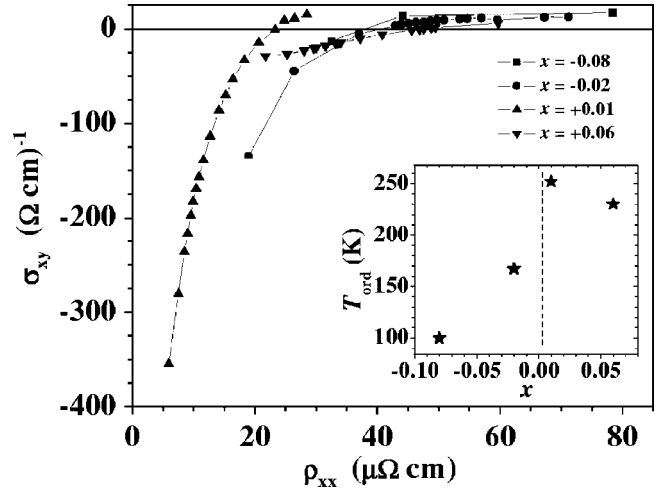


FIG. 5. σ_{xy} vs ρ_{xx} for all samples. Inset: T_{ord} vs x .

of the wave function.¹⁸ It was already demonstrated theoretically that a finite AHE may exist in systems with more than two non-coplanar spin sublattices.¹⁹ Due to the high symmetry of the Fe_3Si system, multiply degenerate contributions to a PHE from the ensemble of possible spin configurations for a given \mathbf{m} will cancel each other out. However, this cancellation, which is also typical for the AHE, may be lifted by topological defects at the boundary between clusters of such configurations²⁰ and by higher-order spin interactions (see Ref. 19 and references therein). Such defects are known to lead to an intrinsic AHE.^{21,22} Also, as shown for other systems,^{6,22} spin orbit interaction will lift these degeneracies, resulting in Berry phase contributions at narrowly defined regions in k space away from the high-symmetry directions considered here.

Another consequence of the spin orbit interaction is a spin scattering asymmetry between different spin sublattices.¹⁹ Defining such a scattering ratio α_i with $i=A, B$, or C , scattering of an electron with momentum \mathbf{p} at a lattice site with an out-of-plane spin component leads to an in-plane field $H_{\text{SO}}^{\text{planar}} \approx \sum_{i=A,B,C} \alpha_i (\mathbf{S}_i \times \mathbf{p})$ which is perpendicular to the electron's momentum \mathbf{p} . In addition, an angular analysis of the spin chirality $\chi_{A,B,C}(\theta_M)$ straightforwardly results in a functional form $H_{\text{SO}}^{\text{planar}} = \sin(\theta_M + \theta) \cos(\theta_M + \theta)$ which corresponds to our experimental observation [see Eq. (4)]. Detailed theoretical calculations beyond the scope of this paper will determine which topological defects and which electrons at the Fermi surface are participating in this angular- and phase-dependent PHE.

Recent calculations⁶ for Fe of the AHE in a Berry phase framework yield a large value $\sigma_{xy} \sim 751$ ($\Omega \text{ cm})^{-1}$ from the saturated magnetization. Accordingly, in the planar Hall geometry, we define σ_{xy} to be

$$\sigma_{xy} = \frac{\Delta \rho_{xy}}{\rho_{xx}^2 + \Delta \rho_{xy}^2}, \quad (5)$$

where $\Delta \rho_{xy} = \rho_{xy}^1 - \rho_{xy}^2$, and ρ_{xy}^1, ρ_{xy}^2 denote the maximum planar Hall resistivities due to the fully saturated magnetiza-

tion (see Fig. 4). For $x=+0.01$ at $T=77$ K, $\sigma_{xy} \sim -350$ ($\Omega \text{ cm}$)⁻¹—an extremely large value compared to AMR theory which suggests an intrinsic magnetotransport regime in our ordered alloy.

As seen in Fig. 1(b), metallic conduction in $\text{Fe}_{3+x}\text{Si}_{1-x}$ is drastically reduced with increasing deviation x from stoichiometry.¹⁴ We may thus *control* structural disorder, while retaining the $D0_3$ crystal structure, and use $\rho_{xx}(T)$ as an ordering parameter. Figure 5 presents the dependence of σ_{xy} on ρ_{xx} for $77 \text{ K} \leq T \leq 300 \text{ K}$. Within $-0.08 \leq x \leq +0.06$, σ_{xy} exhibits two magnetotransport regimes. In the high-temperature regime, i.e., $T > T_{\text{ord}}$, σ_{xy} is of same sign and comparable amplitude $\sim +20$ ($\Omega \text{ cm}$)⁻¹ as for Fe¹² and almost independent of ρ_{xx} . For $T < T_{\text{ord}}$, σ_{xy} changes sign and increases, for low values of x and ρ_{xx} , by over one order of magnitude relative to $\sigma_{xy}(T > T_{\text{ord}})$. No such crossover was observed at $T=4$ K for samples with $x \leq -0.19$ and $x + 0.09$, i.e., farther from $x=0$. In addition, T_{ord} decreases with increasing $|x|$ (see inset of Fig. 5).²³ The T_{ord} range is in good agreement with the exchange energy $J_{\text{ex}}[B \leftrightarrow (A, C)] = 145$ K between Fe(A, C) and Fe(B) sublattices as experimentally determined by Stearns,¹⁷ thus supporting our model. From this we infer that spin-chirality effects between Fe(B) and Fe(A, C) sublattices with coupled spin fluctuations

below T_{ord} drive this *ordered intrinsic* magnetotransport regime. In addition, since only our extension to AMR theory can explain our results above T_{ord} , we presume that similar considerations may apply to this conventional regime at high temperature, in related fashion to the case of Fe.¹²

In conclusion, we have observed an additional contribution to the planar Hall effect through experiments on $\text{Fe}_{3+x}\text{Si}_{1-x}$ films. A microscopic model based on Berry phase effects shows how this extra term reflects magnetic interactions with reduced crystal symmetry for certain Fe sublattices in the ordered Fe_3Si Heusler alloy. Both structural disorder in $\text{Fe}_{3+x}\text{Si}_{1-x}$ across the $-0.08 \leq x \leq +0.06$ stoichiometry range and thermal disorder above a correlated temperature T_{ord} destroy the coherent spin density fluctuations and drive the system into a conventional magnetotransport regime. Our results call for an *ab initio* theory on an intrinsic origin of the planar Hall effect, in particular for Fe_3Si .

We thank A. Riedel for technical assistance, H. T. Grahn for a critical reading of the manuscript, and Y. Takagaki, P. Kleinert, P. K. Muduli, R. Engel-Herbert, and S. L. Lu for stimulating discussions.

*Electronic address: mbowen@pdi-berlin.de

¹T. R. McGuire and R. I. Potter, IEEE Trans. Magn. **11**, 1018 (1975).

²I. A. Campbell and A. Fert, in *Ferromagnetic Materials*, edited by E. P. Wohlfarth (North-Holland, Amsterdam, 1982), Vol. 3, p. 797.

³R. Karplus and J. Luttinger, Phys. Rev. **95**, 1154 (1954).

⁴J. Smit, Physica (Amsterdam) **21**, 877 (1955).

⁵L. Berger, Phys. Rev. B **2**, 4559 (1970).

⁶Y. Yao, L. Kleinman, A. H. MacDonald, J. Sinova, T. Jungwirth, D. S. Wang, E. Wang, and Q. Niu, Phys. Rev. Lett. **92**, 037204 (2004).

⁷M. V. Berry, Proc. R. Soc. London, Ser. A **392**, 45 (1984).

⁸B. Simon, Phys. Rev. Lett. **51**, 2167 (1983).

⁹K.-J. Friedland, R. Nötzel, H. P. Schönherr, A. Riedel, H. Kostial, and K. H. Ploog, Physica E (Amsterdam) **10**, 442 (2000).

¹⁰H. X. Tang, R. K. Kawakami, D. D. Awschalom, and M. L. Roukes, Phys. Rev. Lett. **90**, 107201 (2003).

¹¹T. Jungwirth, Q. Niu, and A. H. MacDonald, Phys. Rev. Lett. **88**, 207208 (2003).

¹²K.-J. Friedland, J. Herfort, P. K. Muduli, H. P. Schönherr, and K.

H. Ploog, J. Supercond. (to be published).

¹³J. Herfort, H.-P. Schönherr, and K. Ploog, Appl. Phys. Lett. **83**, 3912 (2003).

¹⁴J. Herfort, K.-P. Schönherr, K.-J. Friedland, and K. H. Ploog, J. Vac. Sci. Technol. B **22**, 2073 (2004).

¹⁵M. Goto and T. Kamimori, J. Phys. Soc. Jpn. **52**, 3710 (1983).

¹⁶J. Moss and P. J. Brown, J. Phys. F: Met. Phys. **2**, 358 (1972).

¹⁷M. B. Stearns, Phys. Rev. **168**, 588 (1968).

¹⁸J. Ye, Y. B. Kim, A. J. Millis, B. I. Shraiman, P. Majumdar, and Z. Tešanović, Phys. Rev. Lett. **83**, 3737 (1999).

¹⁹R. Shindou and N. Nagaosa, Phys. Rev. Lett. **87**, 116801 (2001).

²⁰Y. Lyanda-Geller, S. H. Chun, M. B. Salamon, P. M. Goldbart, P. D. Han, Y. Tomioka, A. Asamitsu, and Y. Tokura, Phys. Rev. B **63**, 184426 (2001).

²¹Y. Taguchi, Y. Oohara, H. Yoshizawa, N. Nagaosa, and Y. Tokura, Science **291**, 2573 (2001).

²²Z. Fang, N. Nagaosa, K. S. Takahashi, A. Asamitsu, R. Mathieu, T. Ogasawara, H. Yamada, M. Kawasaki, Y. Tokura, and K. Terakura, Science **302**, 92 (2003).

²³The asymmetry in $T_{\text{ord}}(x)$ could reflect the proximity of Fe_3Si to the $D0_3$ phase boundary at $x < 0$. Strain could also play a role.